

Quark deconfinement in compact stars and connection with GRBs

I. Parenti¹, I. Bombaci², I. Vidaña³

¹ Dipartimento di Fisica and INFN of Ferrara, Italy

² Dipartimento di Fisica and INFN of Pisa, Italy

³ Gesellschaft für Schwerionenforschung (GSI), Darmstadt, Germany

Abstract

We study the consequences of the hadron-quark deconfinement phase transition in stellar compact objects when finite size effects between the deconfined quark phase and the hadronic phase are taken into account. We show that above a threshold value of the central pressure (gravitational mass) a neutron star is metastable to the decay (conversion) to a hybrid neutron star or to a strange star. The *mean-life time* of the metastable configuration dramatically depends on the value of the stellar central pressure. We discuss the implications of our scenario on the interpretation of the stellar mass and radius extracted from the spectra of several X-ray compact sources. Finally, we show that our scenario implies, as a natural consequence a two step-process which is able to explain the inferred “delayed” connection between supernova explosions and GRBs, giving also the correct energy to power GRBs.

1 Introduction

One of the most fascinating enigma in modern astrophysics concerns the true nature of the ultra-dense compact objects called neutron stars (NS). The bulk properties and the internal structure of these stars chiefly depends upon the equation of state (EOS) of dense hadronic matter. Different models for the EOS of dense matter predict a neutron star maximum mass (M_{max}) in the range of $1.4 - 2.2 M_{\odot}$, and a corresponding central density in range of $4 - 8$ time the saturation density ($\rho_0 \sim 2.8 \times 10^{14} \text{ g/cm}^3$) of nuclear matter [1, 2]. In the case of a star with $M \sim 1.4M_{\odot}$, different EOS models predict a radius in the range of $7 - 16 \text{ Km}$ [1, 2, 3].

In a simplicist and conservative picture the core of a neutron star is modeled as a uniform fluid of neutron rich nuclear matter in equilibrium with respect to the weak interaction (β -stable nuclear matter). However, due to the large value of the stellar central density and to the rapid increase of the nucleon chemical potentials with density, hyperons

$(\Lambda, \Sigma^-, \Sigma^0, \Sigma^+, \Xi^-$ and Ξ^0 particles) are expected to appear in the inner core of the star. Other exotic phases of hadronic matter such as a Bose-Einstein condensate of negative pion (π^-) or negative kaon (K^-) could be present in the inner part of the star.

According to Quantum Chromodynamics (QCD) a phase transition from hadronic matter to a deconfined quark phase should occur at density of a few times nuclear matter saturation density. Consequently, the core of the more massive neutron stars is one of the best candidates in the Universe where such deconfined phase of quark matter (QM) could be found. This possibility was realized by several researchers soon after the introduction of quarks as the fundamentals building blocks of hadrons [4]. Since β -stable hadronic matter posses two conserved “charges” (*i.e.* electric charge and baryon number) the quark-deconfinement phase transition proceeds through a mixed phase over a finite range of pressures and densities according to the Gibbs’ criterion for phase equilibrium [5]. At the onset of the mixed phase, quark matter droplets from a Coulomb lattice embedded in a sea of hadrons and in a roughly uniform sea of electrons and muons. As the pressure increases various geometrical shapes (rods, plates) of the less abundant phase immersed in the dominant one are expected. Finally the system turns into a uniform quark matter at the highest pressure of the mixed phase [6, 7]. Compact stars which posses a “quark matter core” either as a mixed phase of deconfined quarks and hadrons or a pure quark matter phase are called *Hybrid Neutron Stars* or shortly *Hybrid Stars* (HyS) [8, 9]. In the following of this paper, the more *conventional* neutron stars in which no fraction of quark matter is present, will be referred to a *pure Hadronic Stars* (HS).

Even more intriguing than the existence of a quark core in a neutron star, is the possible existence of a new family of compact stars consisting completely of a deconfined mixture of *up* (*u*), *down* (*d*) and *strange* (*s*) quarks (together with an appropriate number of electrons to guarantee electrical neutrality) satisfying the Bodmer-Witten hypothesis [10, 11]. Such compact stars have been called *strange quark stars* or shortly *strange stars* (SS) [12, 13] and their constituent matter as *strange quark matter* (SQM) [14, 15]. Presently there is no unambiguous proof about the existence of strange stars, however, a size amount of observational data collected by the new generations of X-ray satellites, is providing a growing body of evidence for their possible existence [16, 17, 18, 19]. It is generally believed that the unambiguous identification of a strange star will imply that all pulsars must be strange stars. In the present work we argue that the possible existence of strange stars does not conflict with the existence of *conventional* neutron stars (pure Hadronic Stars).

In this work (based on [20] we study the effects of the hadron-quark deconfinement phase transition in stellar compact objects. We show that when finite size effects at the inter-

face between the quark and the hadron phase are taken into account, pure Hadronic Stars, above a threshold value of the central pressure (and then of the gravitational mass), are metastable to the *decay (conversion)* to hybrid neutron stars or to strange stars (depending on the properties of EOS for quark matter). The *mean-life time* of the metastable stellar configuration is related to the quantum nucleation time to form a drop of quark matter in the stellar center, and dramatically depends on the value of the stellar central pressure. We explore the implications of the metastability of “massive” pure hadronic Stars and the existence of stable compact quark stars (hybrid neutron stars or strange stars) in the interpretation of the mass-radius constraints extracted from the spectra of several X-ray compact sources and we discuss the implications of our scenario for Gamma Ray Bursts.

2 Quantum nucleation of quark matter in hadronic stars

Nucleation of quark matter in neutron stars has been studied by many authors. Most of the earlier studies on this subject [21] have been restricted to the case of thermal nucleation in hot and dense hadronic matter. In these studies, it was found that the prompt formation of a critical size drop of quark matter via thermal activation is possible above a temperature of about 2-3 MeV. As a consequence, it was inferred that pure hadronic stars are converted to strange stars or to hybrid stars within the first second after their birth. It was also suggested that the large amount of energy liberated in this process could play a crucial role in type-II supernova explosions [22].

All the studies on quark matter nucleation mentioned above, have neglected an important physical aspect which characterizes dense matter in a newly born *neutron star*: the trapping of neutrinos in the stellar core. Neutrino trapping has a sizeable influence on the *stiffness* of the EOS and, consequently, on the structural properties of the protoneutron star [23, 24]. In particular, it has been found that neutrino trapping significantly shifts the critical baryon density for the quark deconfinement phase transition to higher values with respect to the neutrino-free case [24, 25]. In addition, neutrino trapping decreases the value of the central density of the stellar maximum mass configuration with respect to the neutrino-free case [24]. Thus, the formation of a metastable supercompressed phase of hadronic matter is strongly inhibited in a protoneutron star.

In the present work, we assume that the compact star survives the early stages of its evolution as a pure hadronic star, and we study quark matter nucleation in cold ($T=0$) neutrino-free hadronic matter.

In bulk matter the quark-hadron mixed phase begins at the *static transition point* defined according to the Gibbs' criterion for the phase equilibrium

$$\mu_H = \mu_Q \equiv \mu_0, \quad P_H(\mu_0) = P_Q(\mu_0) \equiv P_0 \quad (1)$$

where

$$\mu_H = \frac{\varepsilon_H + P_H}{n_{b,H}}, \quad \mu_Q = \frac{\varepsilon_Q + P_Q}{n_{b,Q}} \quad (2)$$

are the chemical potentials for the hadron and quark phase respectively, $\varepsilon_H(\varepsilon_Q)$, $P_H(P_Q)$ and $n_{b,H}(n_{b,Q})$ denote respectively the total (*i.e.*, including leptonic contributions) energy density, the total pressure and baryon number density for the hadron (quark) phase, in the case of cold matter.

Let us consider the more realistic situation in which one takes into account the energy cost due to finite size effects in creating a drop of deconfined quark matter in the hadronic environment. As a consequence of these effects, the formation of a critical-size drop of QM is not immediate and it is necessary to have a overpressure $\Delta P = P - P_0$ with respect to the static transition point. Thus, above P_0 , hadronic matter is in a metastable state, and the formation of a real drop of quark matter occurs via a quantum nucleation mechanism. A sub-critical (virtual) droplet of deconfined quark matter moves back and forth in the potential energy well separating the two matter phases (see discussion below) on a time scale $\nu_0^{-1} \sim 10^{-23}$ seconds, which is set by the strong interactions. This time scale is many orders of magnitude shorter than the typical time scale for the weak interactions, therefore quark flavor must be conserved during the deconfinement transition. We will refer to this form of deconfined matter, in which the flavor content is equal to that of the β -stable hadronic system at the same pressure, as the Q^* -phase. Soon afterwards a critical size drop of quark matter is formed the weak interactions will have enough time to act, changing the quark flavor fraction of the deconfined droplet to lower its energy, and a droplet of β -stable SQM is formed (hereafter the Q -phase). For example, if quark deconfinement occurs in β -stable nuclear matter (non-strange hadronic matter), it will produce a two-flavor (u and d) quark matter droplet having

$$n_u/n_d = (1 + x_p)/(2 - x_p), \quad (3)$$

n_u and n_d being the *up* and *down* quark number densities respectively, and x_p the proton fraction in the β -stable hadronic phase. In the more general case in which the hadronic phase has a strangeness content (*e.g.*, hyperonic matter), the deconfinement transition will

form a droplet of strange matter with a flavor content equal to that of the β -stable hadronic system at the same pressure, according to the relation:

$$\begin{pmatrix} Y_u \\ Y_d \\ Y_s \end{pmatrix} = \begin{pmatrix} 2 & 1 & 1 & 2 & 1 & 0 & 1 & 0 \\ 1 & 2 & 1 & 0 & 1 & 2 & 0 & 1 \\ 0 & 0 & 1 & 1 & 1 & 1 & 2 & 2 \end{pmatrix} \begin{pmatrix} Y_p \\ Y_n \\ Y_\Lambda \\ Y_{\Sigma^+} \\ Y_{\Sigma^0} \\ Y_{\Sigma^-} \\ Y_{\Xi^0} \\ Y_{\Xi^-} \end{pmatrix}$$

where $Y_i = n_i/n_b$ are the concentrations of the different particle species.

In the present work, we have adopted rather common models for describing both the hadronic and the quark phase of dense matter. For the hadronic phase we used models which are based on a relativistic lagrangian of hadrons interacting via exchange of sigma, rho and omega mesons. The parameters adopted are the standard ones [26]. Hereafter we refer to this model as the GM equation of state (EOS). For the quark phase we have adopted a phenomenological EOS [14] which is based on the MIT bag model for hadrons. The parameters here are: the mass m_s of the strange quark, the so-called pressure of the vacuum B (bag constant) and the QCD structure constant α_s . For all the quark matter model used in the present work, we take $m_u = m_d = 0$, $m_s = 150$ MeV and $\alpha_s = 0$.

In the Fig.1 we show the chemical potentials, defined according to Eq.2 as a function of the total pressure for the three phases of matter (H, Q, and Q*) discussed above.

3 Nucleation time

To calculate the nucleation rate of quark matter in the hadronic medium we use the Lifshitz-Kagan quantum theory [27] in the relativistic form given by Iida & Sato (1997) [28]. The QM droplet is supposed to be a sphere of radius R and its quantum fluctuations are described by the lagrangian:

$$L(R, \dot{R}) = -M(R)c^2\sqrt{1 - (\dot{R}/c)^2} + M(R)c^2 - U(R), \quad (4)$$

where $M(R)$ is the effective mass of the QM droplet, and $U(R)$ its potential energy. Within the Lifshitz-Kagan quantum nucleation theory, one assumes that the phase boundary (*i.e.* the droplet surface) moves slowly compared to the high sound velocity of the medium ($\dot{R} \ll v_s \sim c$). Thus the number density of each phase adjust adiabatically to the fluctuations

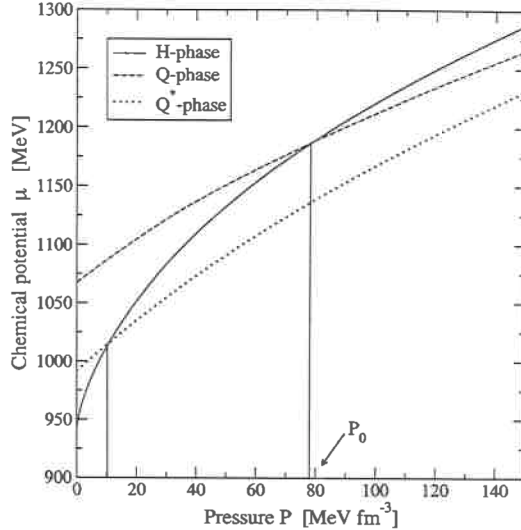


Figure 1: Chemical potential of the three phases of matter (H, Q, and Q*), as defined by Eq. 2 as a function of the total pressure. The hadronic phase is described with the GM3 model whereas for the Q and Q* phases is employed the MIT-like bag model with $m_s = 150$ MeV, $B = 98,83$ MeV/fm 3 and $\alpha_s = 0$. P_0 denote the static transition point.

of the droplet radius, and the system retains pressure equilibrium between the two phases. Thus, the droplet effective mass is given by [27, 28]

$$M(R) = 4\pi\rho_H \left(1 - \frac{n_{b,Q^*}}{n_{b,H}}\right)^2 R^3, \quad (5)$$

ρ_H being the hadronic mass density, n_{b,Q^*} and $n_{b,H}$ are the baryonic number densities at the same pressure in the hadronic and Q*-phase, respectively. The potential energy is given by [27, 28]

$$U(R) = \frac{4}{3}\pi R^3 n_{b,Q^*} (\mu_{Q^*} - \mu_H) + 4\pi\sigma R^2 \quad (6)$$

where μ_H and μ_{Q^*} are the hadronic and quark chemical potentials at a fixed pressure P and σ is the surface tension for the surface separating the quark phase from the hadronic phase. The value of the surface tension σ is poorly known, and typical values used in the literature range within 10-50 MeV/fm 2 [6, 28].

The droplet of deconfined matter is characterized by a critical radius of:

$$R_c = \frac{3\sigma}{n_{b,Q^*}(\mu_H - \mu_{Q^*})} \quad (\text{such that } U(R_c) = 0) \quad (7)$$

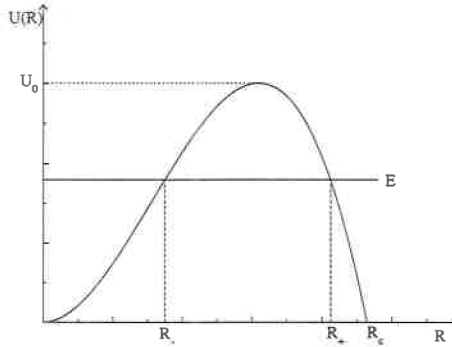


Figure 2: Potential energy of the QM drop as a function of the radius of the drop. U_0 is the maximum width of the barrier, R_c is the critical radius and R_{\pm} are the turning points.

while the maximum width of the barrier is:

$$U_0 = \frac{4}{27} 4\pi\sigma R_c^2 \quad (8)$$

The process of formation of a bubble having a critical radius, can be computed using a semiclassical approximation. The procedure is rather straightforward. First one computes, using the well known Wentzel-Kramers-Brillouin (WKB) approximation, the ground state energy E_0 and the oscillation frequency ν_0 of the virtual QM drop in the potential well $U(R)$. Then it is possible to calculate in a relativistic framework the probability of tunneling as [28]

$$p_0 = \exp \left[-\frac{A(E_0)}{\hbar} \right] \quad (9)$$

where A is the action under the potential barrier

$$A(E) = \frac{2}{c} \int_{R_-}^{R_+} \{ [2M(R)c^2 + E - U(R)] \times [U(R) - E] \}^{1/2} dR \quad (10)$$

R_{\pm} being the classical turning points (see Fig.2).

The nucleation time is then equal to

$$\tau = (\nu_0 p_0 N_c)^{-1}, \quad (11)$$

where N_c is the number of virtual centers of droplet formation in the innermost region of the star. Following the simple estimate given by Iida & Sato [28] we take $N_c = 10^{48}$. The uncertainty in the value of N_c is expected to be within one or two orders of magnitude. In any case, all qualitative features of our scenario will be not affected by the uncertainty in any value of N_c .

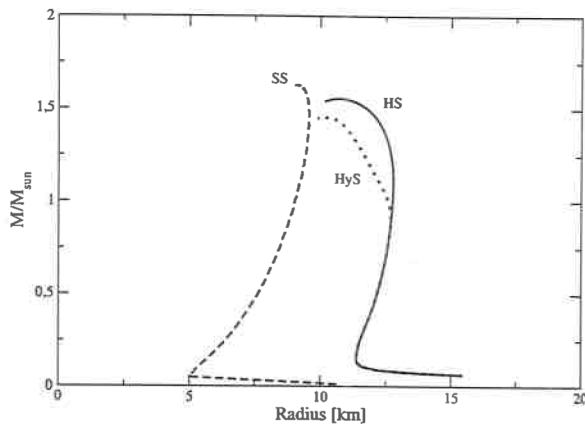


Figure 3: Mass-radius relations for the three types of compact objects discussed in the text: Hadronic Star (HS), Hybrid Star (HyS) and Strange Star (SS). The hadronic phase is described with the GM3 model while the pure quark phase is described by the MIT-like bag model with $m_u = m_d = 0$, $m_s = 150$ MeV, $\alpha_s = 0$ and $B = 136.62(69.47)$ MeV/fm 3 for the hybrid star (strange star).

4 Results

To begin with we show in Fig. 3 the typical mass-radius (MR) relations for the three possible types of compact stars discussed before.

The curve labeled with HS represents the MR relation for pure hadronic stars containing an hyperonic core obtained with the GM3 model for the EOS of dense matter. The curve labeled HyS depicts the MR relation for hybrid neutron stars where the hadronic phase is described by the same GM3 model for the EOS and the quark phase by the MIT-bag like model with $B = 136.62$ MeV/fm 3 . Finally, if we assume, for example, $B = 69.47$ MeV/fm 3 (with the remaining parameters for quark phase unchanged with respect to the previous case), SQM fulfills the Bodmer-Witten hypothesis and one has the strange star sequence depicted by the curve SS in Fig. 3. As it appears, stars having a deconfined quark content (HyS or SS) are more compact than purely hadronic stars (HS).

In our scenario, we consider a purely hadronic star whose central pressure is increasing due to spin-down or due to mass accretion, *e.g.*, from the material left by the supernova explosion (fallback disc), from a companion star or from the interstellar medium. As the central pressure exceeds the threshold value P_0 at the static transition point, a virtual drop of quark matter in the Q*-phase can be formed in the central region of the star. As soon as a real drop of Q*-matter is formed, it will grow very rapidly and the original Hadronic

Star will be converted to and Hybrid Star or to a Strange Star, depending on the detail of the EOS for quark matter employed to model the phase transition (particularly depending on the value of the parameter B within the model adopted in the present study).

The nucleation time τ , *i.e.*, the time needed to form a critical droplet of deconfined quark matter, can be calculated for different values of the stellar central pressure P_c which enters in the expression of the energy barrier in Eq.6. The nucleation time can be plotted as a function of the gravitational mass M_{HS} of the HS corresponding to the given value of the central pressure, as implied by the solution of the Tolmann-Oppeneimer-Volkov equations for the pure Hadronic Star sequences. The results of our calculations (with the GM3 parametrization for the hadronic phase) are reported in Fig. 4. Each curve refers to a different value of the bag constant and the surface tension.

As we can see, from the results in Fig. 4, a metastable hadronic star can have a mean-life time many orders of magnitude larger than the age of the universe $T_{univ} = (13.7 \pm 0.2) \times 10^9$ yr = $(4.32 \pm 0.06) \times 10^{17}$ s [29]. As the star accretes a small amount of mass (of the order of a few per cent of the mass of the sun), the consequential increase of the central pressure lead to a huge reduction of the nucleation time and, as a result, to a dramatic reduction of the HS *mean-life time*.

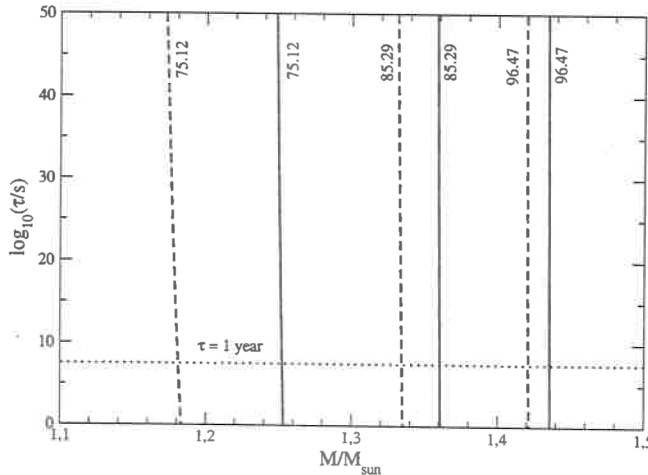


Figure 4: Nucleation time as a function of the gravitational mass of the hadronic star. Solid lines correspond to a value of $\sigma = 30$ MeV/fm 2 whereas dashed ones are for $\sigma = 10$ MeV/fm 2 . The nucleation time corresponding to one year is shown by the dotted horizontal line. The different values of the bag constant (in units of MeV/fm 3) are plotted next to each curve. The hadronic phase is described with the GM3 model.

To summarize, in the present scenario pure hadronic stars having a central pressure larger than the static transition pressure for the formation of the Q^* -phase are metastable to the “decay” (conversion) to a more compact stellar configuration in which deconfined quark matter is present (*i.e.*, HyS or SS). These metastable HS have a *mean-life time* which is related to the nucleation time to form the first critical-size drop of deconfined matter in their interior (the actual *mean-life time* of the HS will depend on the mass accretion or on the spin-down rate which modifies the nucleation time via an explicit time dependence of the stellar central pressure).

We define as *critical mass* M_{cr} of the metastable HS, the value of the gravitational mass for which the nucleation time is equal to one year: $M_{cr} \equiv M_{HS}(\tau = 1\text{yr})$.

Pure hadronic stars with $M_H > M_{cr}$ are very unlikely to be observed. M_{cr} plays the role of an *effective maximum mass* for the hadronic branch of compact stars (see the discussion in section 4). While the Oppenheimer–Volkov maximum mass $M_{HS,max}$ [30] is determined by the overall stiffness of the EOS for hadronic matter, the value of M_{cr} will depend in addition on the bulk properties of the EOS for quark matter and on the properties at the interface between the confined and deconfined phases of matter (*e.g.*, the surface tension σ).

To explore how the outcome of our scenario depends on the details of the stellar matter EOS, we have considered many value of the bag constant B with the same parametrization for the hadronic phase (GM3). Moreover, we have considered two different values for the surface tension: $\sigma = 10 \text{ MeV/fm}^2$ and $\sigma = 30 \text{ MeV/fm}^2$. These results are summarized in Tab. 1.

In Fig.5, we show the MR curve for pure HS within the GM3 model for the EOS of the hadronic phase, and that for hybrid stars or strange stars for different values of the bag constant B .

The configuration marked with an asterisk on the hadronic MR curves represents the hadronic star for which the central pressure is equal to P_0 . The full circle on the hadronic star sequence represents the critical mass configuration, in the case $\sigma = 30 \text{ MeV/fm}^2$.

The full circle on the HyS (SS) mass-radius curve represents the hybrid (strange) star which is formed from the conversion of the hadronic star with $M_{HS} = M_{cr}$.

We assume [31] that during the stellar conversion process the total number of baryons in the star (or in other words the stellar baryonic mass) is conserved. Thus the total energy liberated in the stellar conversion is given by the difference between the gravitational mass of the initial hadronic star ($M_{in} \equiv M_{cr}$) and that of the final hybrid or strange stellar

Table 1: Critical masses and energy released in the conversion process of an HS into a QS for several values of the Bag constant and the surface tension. Column labelled $M_{QS,max}$ ($M_{QS,max}^b$) denotes the maximum gravitational (baryonic) mass of the final QS sequence. The value of the critical gravitational (baryonic) mass of the initial HS is reported on column labelled M_{cr} (M_{cr}^b) whereas those of the mass of the final QS and the energy released in the stellar conversion process are shown on columns labelled M_{fin} and E_{conv} respectively. BH denotes those cases in which due to the conversion the initial HS collapses into a black hole. Units of B and σ are MeV/fm³ and MeV/fm² respectively. All masses are given in solar mass units and the energy released is given in units of 10^{51} erg. The hadronic phase is described with the GM3 model, m_s and α_s are always taken equal to 150 MeV and 0 respectively. The situations for which there is no deconfinement phase transition, or for which the nucleation time of the hadronic maximum mass configuration is of the order or larger than the age of the universe (see discussion in the text) are reported with no entry (-). The maximum mass for the pure HS predicted by the GM3 model is 1.552 M_\odot .

B	$M_{QS,max}$	$M_{QS,max}^b$	$\sigma = 10$				$\sigma = 30$			
			M_{cr}	M_{cr}^b	M_{fin}	E_{conv}	M_{cr}	M_{cr}^b	M_{fin}	E_{conv}
136.63	1.448	1.613	-	-	-	-	1.551	1.734		BH
122.07	1.430	1.600	-	-	-	-	1.539	1.718		BH
108.70	1.440	1.627	1.484	1.648	BH		1.498	1.665		BH
106.17	1.445	1.637	1.474	1.635	1.444	53.4	1.487	1.651		BH
103.68	1.451	1.648	1.461	1.619	1.430	56.2	1.475	1.636	1.442	57.9
101.23	1.458	1.661	1.449	1.603	1.415	59.3	1.462	1.620	1.428	60.9
98.83	1.466	1.676	1.435	1.587	1.400	62.5	1.449	1.604	1.413	64.3
96.47	1.475	1.692	1.421	1.569	1.384	66.3	1.436	1.587	1.398	68.0
94.15	1.485	1.710	1.406	1.550	1.367	70.0	1.422	1.570	1.382	71.9
91.87	1.497	1.731	1.390	1.531	1.348	74.2	1.407	1.552	1.365	76.2
89.64	1.509	1.753	1.373	1.510	1.329	78.5	1.392	1.534	1.347	80.8
87.45	1.523	1.778	1.355	1.488	1.308	83.1	1.376	1.515	1.329	85.7
85.29	1.538	1.804	1.335	1.463	1.285	87.8	1.360	1.495	1.310	90.6
80.09	1.582	1.881	1.270	1.385	1.214	98.7	1.314	1.438	1.255	104.0
75.12	1.631	1.966	1.181	1.280	1.121	107.8	1.252	1.365	1.187	116.85
65.89	1.734	2.155	0.943	1.005	0.877	117.8	1.126	1.216	1.045	144.5
63.12	1.770	2.222	0.808	0.854	0.747	110.2	1.082	1.164	0.997	152.1
59.95	1.814	2.305	0.513	0.531	0.471	74.7	1.010	1.081	0.923	155.5

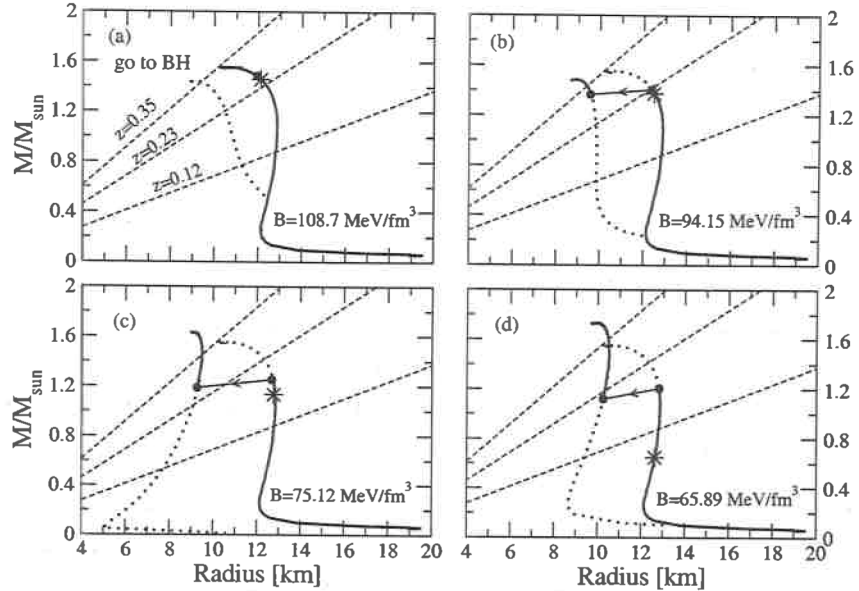


Figure 5: Mass-radius relation for a pure HS described within the GM3 model and that of the HyS or SS configurations for several values of the Bag constant and $m_s = 150$ MeV and $\alpha_s = 0$. The configuration marked with an asterisk represents in all cases the HS for which the central pressure is equal to P_0 . The conversion process of the HS, with a gravitational mass equal to M_{cr} , into a final HyS or SS is denoted by the full circles connected by an arrow. In all the panels σ is taken equal to 30 MeV/fm 2 . The dashed lines show the gravitational red shift deduced for the X-ray compact sources EXO 0748-676 ($z = 0.35$) and 1E 1207.4-5209 ($z = 0.12 - 0.23$).

configuration with the same baryonic mass ($M_{fin} \equiv M_{QS}(M_{cr}^b)$):

$$E_{conv} = (M_{in} - M_{fin})c^2. \quad (12)$$

The stellar conversion process, described so far, will start to populate the new branch of quark stars (the part of the QS sequence plotted as a continuous curve in Fig. 5). Long term accretion on the QS can next produce stars with masses up to the limiting mass $M_{QS,max}$ for the quark star configurations.

5 Mass-to-radius ratio and internal constitution of compact stars

An accurate measure of the radius and the mass of an individual “neutron star” will represent the key to discriminate between different models for the EoS of dense hadronic matter.

Unfortunately such a crucial information is still not available. A decisive step in such a direction has been done thanks to the instruments on board of the last generation of X-ray satellites. These are providing a large amount of fresh and accurate observational data, which are giving us the possibility to extract very tight constraints on the radius and the mass for some compact stars.

The analysis of different astrophysical phenomena associated with compact X-ray sources, seems to indicate in some case the existence of neutron stars with “large” radii (12 – 20 km) and in some other cases the existence of compact stars with “small” radii (6 – 9 km) [16, 18, 32, 33]. Clearly, this possibility is a natural outcome of our scenario, where two different families of compact stars, the pure hadronic stars and the quark stars (HyS or SS), may exist in the universe.

In the following of this section, we will consider some of the most recent constraints on the mass-to-radius ratio for compact stars extracted from the observational data for a few X-ray sources, and we will try make an interpretation of these results within our scenario.

In Fig. 6 we report the radius and the mass of the compact star RX J1856.5-3754 inferred by [34] (see also [35]) from the fit of the full spectral energy distribution for this isolated radio-quite “neutron star”, after a revised parallax determination [35] which implies a distance to the source of 117 ± 12 pc. Comparing the mass-radius box for RX J1856.5-3754 reported in Fig. 6 with the theoretical determination of the MR relation for different equations of state, one concludes that RX J1856.5-3754 could be (see *e.g.* Fig. 2 in [34]) either an hadronic star or an hybrid or strange star (see also [19]).

Next we consider the compact star in the low mass X-ray binary 4U 1728-34. In a very recent paper Shaposhnikov [36] (hereafter STH) have analyzed a set of 26 Type-I X-ray bursts for this source. The data were collected by the Proportional Counter Array on board of the Rossi X-ray Timing Explorer (RXTE) satellite. For the interpretation of these observational data Shaposhnikov used a model of the X-ray burst spectral formation developed by Titarchuk [37]. Within this model, STH were able to extract very stringent constrain on the radius and the mass of the compact star in this bursting source. The radius and mass for 4U 1728-34, extracted by STH for different best-fits of the burst data, are depicted in Fig. 6 by the filled squares. Each of the four MR points is relative to a different value of the distance to the source ($d = 4.0, 4.25, 4.50, 4.75$ kpc, for the fit which produces the smallest values of the mass, up to the one which gives the largest mass). The error bars on each point represent the error contour for 90% confidence level. It has been pointed out [33] that the semi-empirical MR relation for the compact star in 4U 1728-34 obtained by STH is not compatible with models pure hadronic stars, while it is consistent with strange stars or

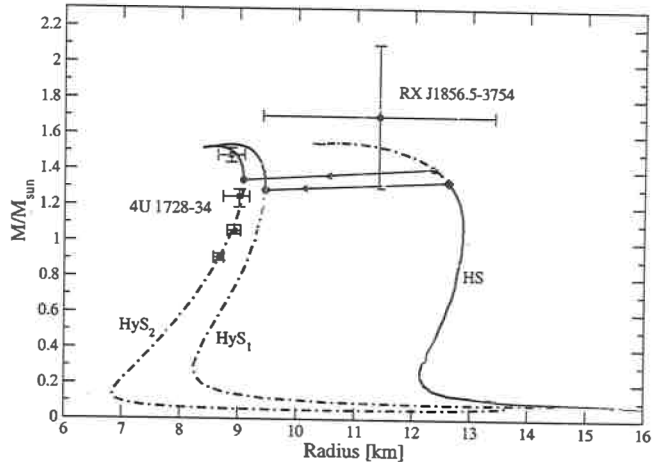


Figure 6: The radius and the mass for RX J1856.5-3754 (full circle with error bars) obtained by [34]. The radius and mass for 4U 1728-34, extracted by [36], is shown by the filled circles with error bars. The curves labeled HS represents the MR relation for pure hadronic star with the GM3 equation of state. The curves labeled HyS₁ and HyS₂ are the MR curves for hybrid stars with the GM3+Bag model EOS, for $B = 85.29 \text{ MeV/fm}^3$ and $m_s = 150 \text{ MeV}$ (HyS₁), and $B = 100 \text{ MeV/fm}^3$ and $m_s = 0 \text{ MeV}$ (HyS₂). The full circles and diamonds on the MR curves represent the critical mass configuration (symbols on the HS curve) and the corresponding hybrid star configurations after the stellar conversion process (symbols on the HyS₁ and HyS₂ curves).

hybrid stars.

Assuming RX J1856.5-3754 to be a pure hadronic star and 4U 1728-34 an hybrid or a strange star, we see from our results plotted in Fig. 6, that this possibility can be realized as a natural consequence of our scenario. Thus, we find that the existence of quark stars (with “small” radii) does not exclude the possible existence of pure hadronic stars (with “large” radii), and *vice versa*.

Decisive informations on the mass-to-radius ratio can be provided by measuring the gravitational redshift of lines in the spectrum emitted from the compact star atmosphere. Very recently, redshifted spectral lines features have been reported for two different X-ray sources [38, 41]. The first of these sources is the compact star in the low mass X-ray binary EXO 0748-676. Studing the spectra of 28 type-I X-ray bursts in EXO 0748-676, Cottam et al. [38] have found absorption spectral line features, which they identify as signatures of Fe XXVI (25-time ionized hydrogen-like Fe) and Fe XXV from the $n = 2 \rightarrow 3$ atomic transition, and of O VIII ($n = 1 \rightarrow 2$ transition). All of these lines are redshifted, with a

unique value of the redshift $z = 0.35$. Interpreting the measured redshift as due to the strong gravitational field at the surface of the compact star (thus neglecting general relativistic effects due to stellar rotation on the spectral lines [39], one obtains a relation for the stellar mass-to-radius ratio:

$$M/M_{\odot} = \left(1 - \frac{1}{(z+1)^2}\right) R/R_{g\odot}, \quad (13)$$

($R_{g\odot} = 2GM_{\odot}/c^2 = 2.953$ km) which is reported in Fig. 5 as a dashed line labeled $z = 0.35$. Comparing with the theoretical MR relations for different EOS (see e.g. Fig.5, and also [40]) it is clear that all three possible families of compact stars discussed in the present paper are completely consistent with a redshift $z = 0.35$.

The second source for which it has been claimed the detection of redshifted spectral lines is 1E 1207.4-5209, a radio-quiet compact star located in the center of the supernova remnant PSK 1209-51/52. 1E 1207.4-5209 has been observed by the Chandra X-ray observatory. Two absorption features have been detected in the source spectrum and have been interpreted [41] as spectral lines associated with atomic transitions of once-ionized helium in the atmosphere of a strong magnetized ($B \sim 1.5 \times 10^{14}$ G) compact star. This interpretation gives for the gravitational redshift at the star surface $z = 0.12 - 0.23$ [41], which is reported in Fig. 5 by the two dashed lines labeled $z = 0.12$ and $z = 0.23$.

How it is possible to reconcile the gravitational redshift $z = 0.12 - 0.23$ for 1E 1207.4-5209 with that ($z = 0.35$) deduced for EXO 0748-676? Within the commonly accepted view, in which there exist in nature only one family of compact stars (the “neutron stars”), different values of the gravitational redshift could be a consequence of a different mass of the two stars. In our scenario, we can give a different interpretation: 1E 1207.4-5209 is a pure hadronic star whereas EXO 0748-676 is an hybrid star or a strange star. This is illustrated in Fig. 5 by comparing our calculated MR relations with the redshifts deduced for the two compact X-ray sources.

6 Quark Deconfinement Nova and GRBs

A large variety of observational data are giving a mounting evidence that “long-duration” Gamma Ray Bursts (GRBs) are associated with supernova explosions [42, 43, 44, 45, 46]. Particularly, in the case of the gamma ray burst of July 5, 1999 (GRB990705), in the case of GRB020813 and of GRB011211, it has been possible to estimate the time delay between the two events.

For GRB990705 [42] evaluated that the supernova explosion (SNE) has occurred about 10 years before the GRB, while [47], giving a different interpretation of the same observational

data, deduced a time delay of about one year. In the case of GRB020813 the supernova event has been estimated [48] to have occurred a few months before the GRB, while in the case of GRB011211 about four days before the burst [44]. If a time-delay between a SNE and the associated GRB will be confirmed by further and more accurate observations, thus it is necessary to have a two-step process. The first of these process is the supernova explosion which forms a compact stellar remnant, *i.e.* a neutron star. The second catastrophic event is associated with the neutron star and it is the energy source for the observed GRB. These new observational data, and the two-step scenario outlined above, poses severe problems for most of the current theoretical models for the central energy source (the so called “central engine”) of GRBs.

In a recent paper Berezhiani et al. (2003) [49] have given a simple and natural interpretation of the “delayed” Supernova-GRB connection in terms of the stellar conversion model (hereafter the *Quark Deconfinement Nova* (QDN)) discussed in the present work. In an other paper Drago et al. [50] exploring the case in which the color superconductivity is taken into account. Here, with respect to [49], we have calculated the nucleation time by considering the quantum tunneling of a virtual drop of quark matter in the so called Q^* -phase (see sect. 2), contrary to [49] where quark flavor conservation during the deconfinement transition has been neglected. We have verified that flavor conservation in computing the nucleation time produces sizable differences in the value of the critical mass M_{cr} and on the energy released during the QDN which powers the GRB.

As we can see from the results reported in Tab. 1, the total energy (E_{conv}) liberated during the stellar conversion process is in the range $0.5\text{--}1.7 \times 10^{53}$ erg. This huge amount of energy will be mainly carried out by the neutrinos produce during the stellar conversion process. It has been pointed out by [51] that near the surface of a compact stellar object, due to general relativity effects, the efficiency of the neutrino-antineutrino annihilation into e^+e^- pairs is strongly enhanced with respect to the Newtonian case, and it could be as high as 10%. The total energy deposited into the electron-photon plasma can therefore be of the order of $10^{51}\text{--}10^{52}$ erg.

The strong magnetic field of the compact star will affect the motion of the electrons and positrons, and in turn could generate an anisotropic γ -ray emission along the stellar magnetic axis. This picture is strongly supported by the analysis of the early optical afterglow for GRB990123 and GRB021211 [52], and by the recent discovery of an ultra-relativistic outflow from a “neutron star” in a binary stellar system [53]. Moreover, it has been recently shown [54] that the stellar magnetic field could influence the velocity of the “burning front” of hadronic matter into quark matter. This results in a strong geometrical asymmetry of the

forming quark matter core along the direction of the stellar magnetic axis, thus providing a suitable mechanism to produce a collimated GRB [54]. Other anisotropies in the GRB could be generated by the rotation of the star.

7 Summary

In the present work, we have investigated the consequences of the hadron-quark deconfinement phase transition in stellar compact objects when finite size effects between the deconfined quark phase and the hadronic phase are taken into account. We have found that above a threshold value of the gravitational mass a pure hadronic star is metastable to the decay (conversion) to a hybrid neutron star or to a strange star¹.

We have calculated the *mean-life time* of these metastable stellar configurations, the critical mass for the hadronic star sequence, and have explored how these quantities depend on the details of the EOS for dense matter. For a more detailed analysis on the concept of the limiting mass of compact stars refer to [20]. We have demonstrated that, within the astrophysical scenario proposed in the present work, the existence of compact stars with “small” radii (quark stars) does not exclude the existence of compact stars with “large” radii (pure hadronic stars), and *vice versa*.

Finally, we have shown that our scenario implies, as a natural consequence a two step-process which is able to explain the inferred “delayed” connection between supernova explosions and GRBs, giving also the correct energy to power GRBs.

There are various specific features and predictions of the present model, which we briefly mention in the following. The second explosion (*Quark Deconfinement Nova*) take place in a “baryon-clean” environment due to the previous SN explosion. It is possible to have different time delays between the two events since the *mean-life time* of the metastable hadronic star depends on the value of the stellar central pressure. Thus the present model is able to interpret a time delay of a few years (as observed in GRB990705 [42, 47] of a few months (as in the case of GRB020813 [48]), of a few days (as deduced for GRB011211 [44]), or the nearly simultaneity of the two events (as in the case of SN2003 and GRB030329 [45]).

¹ The particular type of quark star (it i.e. hybrid star or strange star) formed at the end of the stellar conversion, will depend on the details of the quark matter EOS (see sect. 3). Here we want to stress that our scenario does not require as a necessary condition the fulfilment of the Bodmer-Witten hypothesis on the absolute stability of strange matter and, thus the existence of strange stars. The delayed stellar conversion process described in this paper takes place also in the case a more “traditional” hybrid star is formed.

References

- [1] S. L. Shapiro & S. A. Teukolsky, *Black holes, white dwarfs and neutron stars* (Ed. J. Wiley & Sons, 1983)
- [2] P. Haensel, *Equation of state of dense matter and maximum mass of neutron stars, in Final Stages of Stellar Evolution* Ed. C. Motch and J.-M. Hameury, EAS Publications Series **7**, 249 (2003)
- [3] M. Dey, I. Bombaci, J. Dey, S. Ray & B. C. Samanta, Phys. Lett. **B438**, 123 (1998); erratum 1999, Phys. Lett. **B467**, 303 (1999)
- [4] N. Itoh, Prog. Theor. Phys. **44**, 291 (1970); G. Baym & S. A. Chin, Phys. Lett. **B62**, 241 (1976)
- [5] N. K. Glendenning, Phys. Rev. **D46**, 1274 (1992); H. Müller & B. D. Serot, Phys. Rev. **C52**, 2072 (1995)
- [6] H. Heiselberg, C. J. Pethick & E. F. Staubo, Phys. Rev. Lett. **70**, 1355 (1993)
- [7] D. N. Voskresensky, M. Yasuhira & T. Tatsumi, Nucl. Phys. **A723**, 291 (2003)
- [8] N. K. Glendenning, *Compact Stars: Nuclear Physics, Particle Physics and General Relativity*, (Springer Verlag, 1996)
- [9] A. Drago & A. Lavagno, Phys. Lett. **B511**, 229 (2001)
- [10] A. R. Bodmer, Phys. Rev. **D4**, 1601 (1971)
- [11] E. Witten, Phys. Rev. **D30**, 272 (1984)
- [12] C. Alcock, E. Farhi & A. Olinto, ApJ. **310**, 261 (1986)
- [13] P. Haensel, J. L. Zdunik & R. Schaefer, A&A **160**, 121 (1986)
- [14] E. Farhi & R. L. Jaffe, Phys. Rev. **D30**, 2379 (1984)
- [15] J. Madsen, Lectures Notes in Physics Vol. **500**, Springer Verlag, 162 (1999)
- [16] I. Bombaci, Phys. Rev. **C55**, 1587 (1997)
- [17] K. S. Cheng, Z. G. Dai, D. M. Wai & T. Lu, Science **280**, 407 (1998); X. -D. Li, S. Ray, J. Dey, M. Dey & I. Bombaci, ApJ. **527**, L51 (1999); R. X. Xu, ApJ. **570**, L65 (2002)

[18] X. -D. Li, I. Bombaci, M. Dey, J. Dey & E. P. J. van den Heuvel, Phys. Rev. Lett. **83**, 3776 (1999)

[19] J. J. Drake et al., ApJ. **572**, 996 (2002)

[20] I. Bombaci, I. Parenti, I. Vidaña, ApJ. **614**, 314 (2004)

[21] J. E. Horvath Phys. Rev. **D49**, 5590 (1994); M. L. Olesen & J. Madsen, Phys. Rev. **D49**, 2698 (1994); H. Heiselberg, *in Strangeness and Quark Matter*, World Scientific **338** (1995); F. Grassi, ApJ. **492**, 263 (1998)

[22] O. G. Benvenuto & J. E. Horvath, Phys. Rev. Lett. **63**, 716 (1998)

[23] I. Bombaci, A &A **305**, 871 (1996)

[24] M. Prakash, I. Bombaci, M. Prakash, P. J. Ellis, J. M: Lattimer & R. Knorren, Phys. Rep. **280**, 1 (1997)

[25] G. Lugones & O. G. Benvenuto, Phys. Rev. **D58**, 083001 (1998)

[26] N. K. Glendenning & S. A. Moszkowski, Phys. Rev. Lett. **67**, 2414 (1991)

[27] I. M. Lifshitz & Y. Kagan, Sov. Phys. JETP **35**, 206 (1972)

[28] K. Iida & K. Sato, Prog. Theor. Phys. **1**, 277 (1997): Phys. Rev. **C58**, 2538 (1998)

[29] D. N. Spergel, Astrophys. J. Suppl. **148**, 175 (2003)

[30] J. R. Oppenheimer & G. M. Volkoff, Phys. Rev. **55**, 374 (1939)

[31] I. Bombaci & B. Datta, ApJ. **530**, L69 (2000)

[32] J. Poutanen & M. Gierliński MNRAS **343**, 1301 (2003)

[33] I. Bombaci, astro-ph/0307522 (2003)

[34] F. M. Walter & J. M. Lattimer, ApJ. **576**, L148 (2002)

[35] D. L. Kaplan, M. H. van Kerkwijk & J. Anderson ApJ. **571**, 447 (2002)

[36] N. Shaposhnikov, L. Titarchuk & F. Haberl, ApJ. **593**, L38 (STH) (2003)

[37] L. Titarchuk ApJ. **429**, 330 (1994); N. Shaposhnikov & L. Titarchuk, ApJ. **570**, L25 (2002)

[38] J. Cottam, F. Paerels & M. Mendez, Nature **420**, 51 (2002)

- [39] F. Özel & D. Psaltis, *ApJ.* **582**, L31 (2003)
- [40] R. X. Xu, *Chin. J. Astron. Astrophys.* **3**, 33 (2003)
- [41] D. Sanwal, G. G. Pavlov, V. E. Zavlin & M. A. Teter, *ApJ.* **574**, L61 (2002)
- [42] L. Amati et al., *Science* **290**, 953 (2000)
- [43] J. S. Bloom et al. *Nature* **401**, 453 (1999); L. A. Antonelli et al., *ApJ.* **545**, L39 (2000); L. Piro et al., *Science* **290**, 955 (2000)
- [44] J. N. Reeves et al., *Nature*, **414**, 512 (2002)
- [45] J. Hjorth et al., *Nature* **423**, 847 (2003)
- [46] P. A. Price et al., *Nature* **423**, 844 (2003); K. Z. Stanek et al., *ApJ.* **591**, L17 (2003); Y. M. Lipkin et al., *ApJ.* **606**, 381 (2004)
- [47] D. Lazzati, G. Ghisellini, L. Amati, F. Frontera, M. Vietri & L. Stella, *ApJ.* **556**, 471 (2001)
- [48] N. R. Butler et al., *ApJ.* **597**, 1010 (2003)
- [49] Z. Berezhiani, I. Bombaci, A. Drago, F. Frontera & A. Lavagno, *ApJ.* **586**, 1250 (2003)
- [50] A. Drago, A. Lavagno and G. Pagliara, *Phys. Rev.* **D69** (2004)
- [51] J. D. Salmonson & J. R. Wilson, *ApJ.* **517**, 859 (1999)
- [52] B. Zhang, S. Kobayashi & P. Meszaros, *ApJ.* **595**, 950 (2003)
- [53] R. Fender et al. *Nature* **427**, 222 (2004)
- [54] G. Lugones, C. R. Ghezzi, E. M. de Gouveia Dal Pino & J. E. Horvath, *ApJ.* **581**, L101 (2002)